

1 Identification of Major Contributors in Atmospheric Particulate
2 Matters to Oxidative Stress by Using Surrogate Particles

3

4 Keda Zhao^{1,2}, Minjie Li³, Lixia Zhao¹, Nan Sang⁴, Liang-Hong Guo^{5,6*}

5

6

7 ¹Research Center for Eco-environmental Sciences, Chinese Academy of Sciences,
8 Beijing, China

9 ²College of Resources and Environment, University of the Chinese Academy of Sciences,
10 Beijing, China

11 ³College of Quality & Safety Engineering, China Jiliang University, Hangzhou, Zhejiang,
12 China

13 ⁴College of Environment and Resource, Shanxi University, Taiyuan, Shanxi, China

14 ⁵Institute of Environmental and Health Sciences, China Jiliang University, Hangzhou,
15 Zhejiang, China

16 ⁶Institute of Environmental and Health, Jiangnan University, Wuhan, Hubei, China

17

18

19 *Corresponding author. Institute of Environmental and Health Sciences, China Jiliang
20 University, 168 Xueyuan Street, Hangzhou, Zhejiang 310008, China. Email:
21 LHGuo@cjlu.edu.cn.

22

Supporting Information

1. Characterization of surrogate particles

Surface area of the naked and B[a]P-coated carbon black particles was measured on a Micromeritics ASAP2460 BET analyzer (Micromeritics Instrument Corp., Norcross, GA, USA). Zeta potential and hydrodynamic diameter of the particles were measured at 25°C on a Zetasizer Nano analyzer (Malvern Instruments, Malvern, UK).

The result of surface area measurement is listed in Table S1. As the size of CB particle increased, its specific surface area decreased significantly. B[a]P coating reduced the specific surface area of CB14 from 260.4 m²/g to the range of 188.4-207.0 m²/g, but there is no correlation between the amount of BaP adsorption and the reduction in specific surface area. The specific surface area of CB14 here is close to the one in a previous report, as is the reduction of the surface area after BaP coating¹.

When the particles were dispersed in the complete cell culture medium, the hydrodynamic diameters of CB14, CB56 and CB260 are all much larger than their physical size, suggesting adsorption of cell culture components on the particle surface or agglomeration of carbon black particles. These results are also consistent with those reported in previous study².

The zeta potential of all the CB particles in the DMEM medium was about -20mV, and there is no significant difference between different types of CB particles. This is most likely due to the adsorption of the same cell culture components on the particle surface.

For BaP-coated particles, there is a possibility for the desorption of BaP from the particle surface in the suspension. To evaluate its stability, the concentration of free B[a]P in the BaP-coated CB particle suspension was measured as follows. The surrogate CB particles are suspended in the culture medium at a concentration of 1 mg/mL. After one-month incubation in the culture medium, the supernatant is collected by centrifugation at 12000rpm for 30 minutes at 4°C, and extracted with n-hexane 3 times. The content of B[a]P in the supernatant is quantified in GC/MS with 0.5 µg Per-d12 as the internal standard. The concentrations of free B[a]P in CB14-BaP-1, CB14-BaP-2, and CB14-BaP-3 suspension were below the detection limit (lower than 4.5 ng/mL), 0.36 µM (0.092

55 $\mu\text{g/mL}$), and $1.07 \mu\text{M}$ ($0.27 \mu\text{g/mL}$), respectively. Therefore, more than 99% BaP
56 remained on the surface of the particles.

57 **2. Characterization of the abiotic ROS in model particles**

58 The abiotic ROS in model particles was detected with DCFH solution, and
59 experiment conditions were performed as follows ³. Briefly, the DCFH solution was
60 obtained by chemical hydrolysis of DCFH-DA solution by 1 M NaOH in dark for 30min
61 at room temperature ⁴. Then the hydrolysate was neutralized with 0.25 M NaH_2PO_4 to pH
62 7.2. The DCFH solution was prepared immediately before use. Model particles and
63 DCFH were mixed in free-phenol red RPMI 1640 medium, with or without argon
64 bubbled through for 2 min, and the suspension were then sealed in brown bottles. At 0hr
65 and 24hr, the mixtures were transferred into a 96-well plate. And the fluorescence
66 intensity was measured on a Thermo Varioskan Flash microplate reader (Waltham, MA,
67 USA), with an excitation wavelength of 485 nm and an emission wavelength of 535 nm.
68 The fold change of the ROS level was obtained by dividing the fluorescence intensity at
69 the specified time by that at 0 hr.

70 The abiotic ROS in model particles were measured with the fluorescence probe. As
71 shown in Fig. S1A, without argon bubbled through, different CB treatment induced
72 similar level of ROS. And with argon bubbled through, $20 \mu\text{g/mL}$ CB14, CB56 or CB260
73 did not induce significant change of ROS (Fig. S1B), compared with control group.
74 These results indicated that dissolved oxygen in the suspension oxidized the fluorescence
75 probe, DCFH, resulting in an increase in fluorescence intensity, while the particles
76 themselves do not carry ROS.

77 **3. The effect of model particles uptake on ROS generation**

78 To further investigate whether ROS generation was dependent on endocytosis of
79 particles, cells were pretreated with a mix of five endocytosis inhibitors before cell
80 exposure to these model particles. The inhibitors include $2.5 \mu\text{g/mL}$ chlorpromazine
81 (CPZ, an inhibitor of clathrin-mediated endocytosis), 1 mg/mL Methyl- β -cyclodextrin
82 (M β CD, an inhibitor of caveolin), 2.5 mM NaN_3 (an inhibitor of ATP-required
83 endocytosis), 250 μM Amiloride (an inhibitor of micropinocytosis), and $2.5 \mu\text{g/mL}$
84 cytochalasin D (Cyto D, an inhibitor of actin). As can be seen in Fig. S4, these
85 endocytosis inhibitors treatment suppressed CB particle-induced ROS, but not affect the

86 fluorescence intensity of intracellular DCFH, indicating that the decrease of fluorescence
87 change fold was due to the reduction in the uptake of model particles rather than the
88 reduction in the uptake of fluorescence probe.

89

90

92

93 **Table S1.** Results of characterization of the particles

	CB14	CB14-BP1	CB14-BP2	CB14-BP3	CB56	CB260
Particle Size(nm)	14	14	14	14	56	260
Surface Area (m²/g)	260.4	195.1	207.0	188.4	43.1	9.7
Adsorbed B[a]P/CB (mg/g)	n.d.	8.7 (34μmol)	24 (95μmol)	47 (185μmol)	n.d.	n.d.
Free B[a]P/CB (mg/g)	n.d.	n.d. (<4.5ng/mL)	0.092 (0.36μmol)	0.27 (1.1μmol)	n.d.	n.d.
Free B[a]P Percentage (%)	-	0.06	0.38	0.59	-	-
Hydrodynamic diameter (nm)	266.9 ± 7.4	260.0 ± 3.3	428.3 ± 21.9	263.6 ± 6.4	163.1 ± 0.5	464.3 ± 7.6
zeta potential (mV)	-19.50 ± 0.35	-19.73 ± 0.55	-17.4 ± 0.62	-20.50 ± 0.50	-26.37 ± 0.72	-26.60 ± 0.4

94 n.d. means not detected, and the detection limit of B[a]P was 4.5 ng/mL.

95

96

97

98

99

100

101

102

104

105 **Table S2.** The interaction analysis of CB14 and metals effect on A549 cell viability. F
 106 and P values obtained from the two-way ANOVA.

Interaction	F	P	Interaction	F	P
CB14+Zn	0.2137	0.9972	CB14+Al	0.4758	0.9212
CB14+Mn	0.2455	0.9947	CB14+Ni	0.439	0.9035
CB14+Fe	1.523	0.1411	CB14+Cd	0.1481	0.9995
CB14+Cu	0.2646	0.9926	CB14+Cr	0.4738	0.9176

107

108

109

110

111

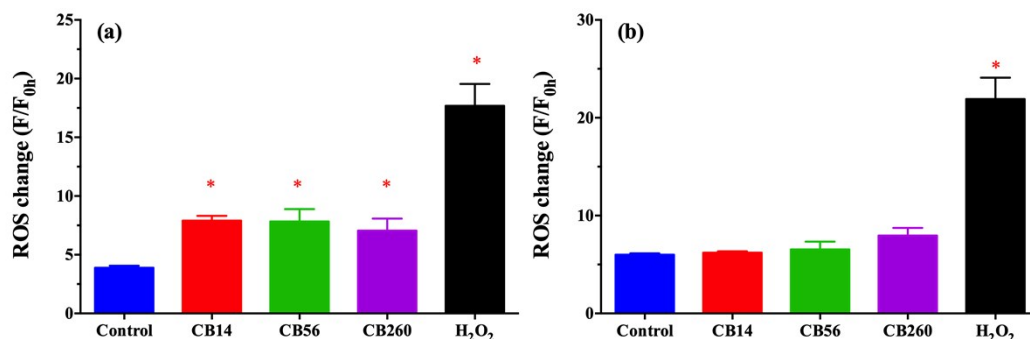
112 **Table S3.** The interaction analysis of CB14 and metals effects on ROS level in A549
 113 cell. F and p values obtained from the two-way ANOVA.

	F (Interaction)	p(Interaction)	E_{A×B}	Type
CB14+Zn	0.020 < 5	> 0.05		Additive
CB14+Mn	15.17 > 5	< 0.05	< E _A +E _B	Antagonistic
CB14+Fe	6.276 > 5	< 0.05	< E _A +E _B	Antagonistic
CB14+Cu	13.21 > 5	< 0.05	< E _A +E _B	Antagonistic
CB14+Al	1.07 < 5	> 0.05		Additive
CB14+Ni	0.481 < 5	> 0.05		Additive
CB14+Cd	0.148 < 5	> 0.05		Additive
CB14+Cr	0.545 < 5	> 0.05		Additive

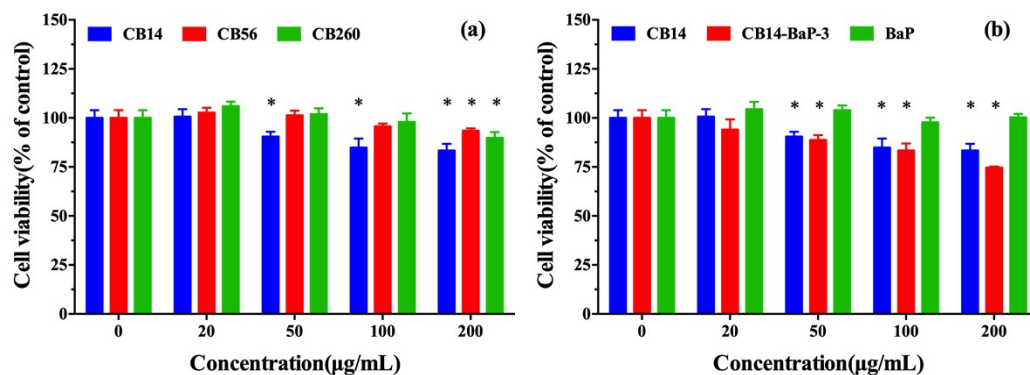
114

115

116



117
 118 **Figure S1.** Fold change of abiotic ROS level in CBs suspensions (20 µg/mL) after 24hr
 119 without (a) or with (b) argon bubbled through. * p < 0.05 compared with control.



123
 124 **Figure S2.** Change of BEAS-2B cell viability after 24hr exposure to (a) CB particles of
 125 different sizes; (b) 14nm CB particles with BaP coating. Results were representative of at
 126 least three independent experiments and expressed as mean \pm S.D. * p < 0.05 compared
 127 with untreated control.

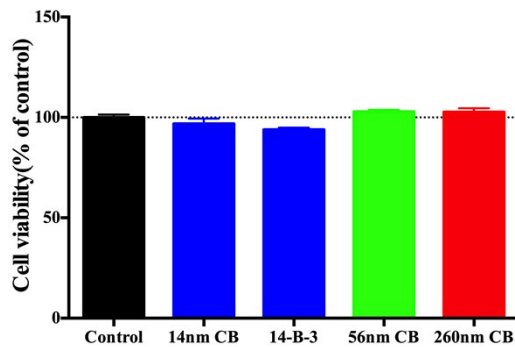


Figure S3. Change of BEAS-2B cell viability after 6hr exposure to four model particles, respectively.

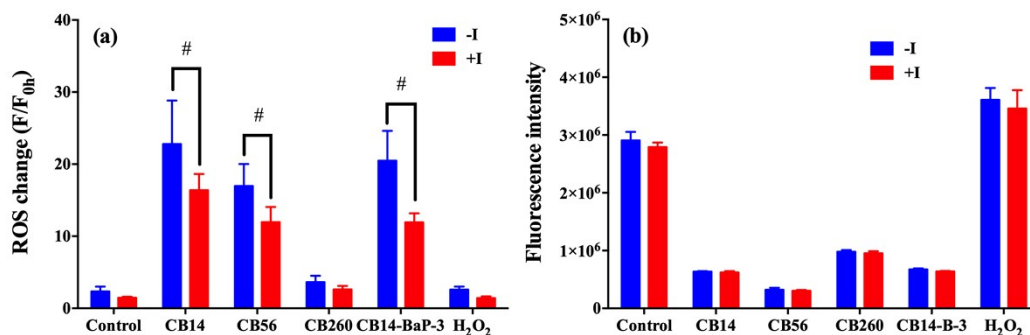


Figure S4. (a) Fold change of ROS level in BEAS-2B cells after 24hr exposure (20 μ g/mL) with or without pretreatment of five inhibitors. (b) Fluorescence intensity of DCFH in BEAS-2B cells after 0hr exposure with or without pretreatment of five inhibitors. Data points represented are mean \pm SD of three parallel experiments. Statistically significant difference from without inhibitors group: # $p < 0.05$.

151 **References**

- 152 1. Lindner K, Stroebele M, Schlick S, et al. Biological effects of carbon black
153 nanoparticles are changed by surface coating with polycyclic aromatic hydrocarbons.
154 *Part Fibre Toxicol* 2017; 14: 8.
- 155 2. Long CM, Nascarella MA, Valberg PA. Carbon black vs. black carbon and other
156 airborne materials containing elemental carbon: Physical and chemical distinctions.
157 *Environmental Pollution* 2013; 181: 271–286.
- 158 3. Foucaud L, Wilson MR, Brown DM, et al. Measurement of reactive species
159 production by nanoparticles prepared in biologically relevant media. *Toxicology*
160 *Letters* 2007; 174: 1–9.
- 161 4. Cathcart R, Schwieters E, Ames BN. Detection of picomole levels of hydroperoxides
162 using a fluorescent dichlorofluorescein assay. *Analytical Biochemistry* 1983; 134:
163 111–116.

164